ISSN 1054-660X, Laser Physics, 2009, Vol. 19, No. 8, pp. 1705–1711.

Suppressed Molecular Ionization due to Interferences Effects[1, *]

A. Jaroń-Becker and A. Becker

JILA and Department of Physics, University of Colorado, Boulder, CO 80309-0440, USA

e-mail: andreasb@jilau1.colorado.edu

Received March 22, 2009

Abstract—The phenomenon of suppressed molecular ionization denotes a number of experimental observations in recent years, in which, in general, the ion yields of a molecule are found to be suppressed as compared to those of its companion atom. The latter are often estimated by the popular tunneling formula given by Ammosov, Delone and Krainov (or ADK). Results of *S*-matrix calculations, obtained for a series of molecules, ranging from diatomics to fullerenes, show that interference effects arising due to the multi-center nature of the molecule contribute to the observed suppression.

PACS numbers: 33.80.Rv, 33.80.Wz, 42.50.Hz

DOI: 10.1134/S1054660X09150201

1. INTRODUCTION

The concept of tunneling ionization has been successfully applied in the context of the interaction of ultrashort intense laser pulses with matter. The phenomenon itself, namely the tunneling of an electron through the potential barrier created by an external (DC) electric field and a Coulomb potential, ranges back to the development of quantum mechanical theories in the early 1930s (see, e.g., [1]). Following the pioneering paper by Keldysh [2] several theoretical approaches to describe strong-field ionization by a slowly alternating electric field (in particular, intense laser pulses) in the quasi-static tunneling limit have been developed in the 1960s (e.g. [3]). The quasi-static tunneling picture is nowadays an important part of our understanding of many basic strong-field processes, ranging from high-order harmonic generation via nonsequential double ionization to attosecond pulse generation.

For atoms the rate of tunneling ionization is often quantified using the so-called ADK formula, given by Ammosov, Delone and Krainov in 1986 [4]. In its simple analytical form the ionization rate (as in other tunneling formula too) depends exponentially on $E_B^{3/2}/E_0$, where E_B is the binding energy of the electron in the undisturbed Coulomb potential of the atom and E_0 is the field strength of the external field. Experiments by Chin and coworkers using CO_2 laser pulses at wavelengths in the far-infrared showed the first evidence of the phenomenon of tunneling ionization of an atom in an intense laser field [5–7]. For the analysis of their experimental data they used the ADK formula. Since then many experimental studies at other wavelengths confirmed the agreement between experiment and ADK theory for the atomic case as long as Keldysh's tunneling criterion is fulfilled. Among others, the ADK formula is nowadays often used to determine saturation intensities of atoms in an experiment.

Although the ADK formula has been derived in its original form for complex but *single-center* objects, i.e. atoms, the simple dependence of the rate on just one target parameter, namely the binding parameter, raised the question whether or not the ionization rate of more complex targets, e.g. small molecules, follow a similar dependence. Data of early experiments with di- and triatomic molecules at CO_2 laser wavelengths (about 10 μm) showed a remarkable agreement between the measured ionization yields and the predictions of the quasistatic ADK tunneling formula [8]. Therefore, it was initially assumed that molecular ionization could be understood in terms of the same tunneling ionization process, in which the ionization probability primarily depends on the binding energy of the electron. More recently, however, strong deviations from this expectation have been discovered in particular at the wavelengths of Ti:sapphire laser systems (about 800 nm). First, Talebpour et al. [9] and Guo et al. [10] have found that although the ionization signal of N_2 is comparable to that of its companion atom Ar (both having almost the same binding energy), as expected in the tunneling ionization picture, the signal of O_2 is strongly *suppressed* as compared to its companion atom Xe. Meanwhile, suppressed ionization has been observed in many molecules, including diatomics [11, 12], hydrocarbons [13–15], biomolecules [16], chlorinated and fluorinated benzenes [17] and the fullerene C_{60} [18]. Therefore, at Ti:sapphire wavelengths suppression of molecular ion yields as compared to the ion yields of a companion atom, or equivalently the predictions of the ADK formula, appears to be a general phenomenon.

What are the characteristic differences between the atomic and molecular case, which cause the suppres-

[1] The article is published in the original.

* We dedicate this article to Prof. N.B. Delone.

sion of the molecular ionization yields and, hence, provide the physical origin of the differences to the atomic tunneling ionization picture, which is the basis of the popular ADK model? In this contribution we review recent theoretical insights in the role of interference effects arising from the multi-center nature of a molecule in this phenomenon. The results are based on the first-order term of the ab-initio S-matrix series [2, 19–21] to investigate the single-active electron ionization of molecules. Good agreement has been found in the past between the theoretical predictions and experimental data for the diatomics N_2 and O_2 [22], a couple of hydrocarbons [23], and fullerenes [24, 25]. In the analysis of the theoretical results it has been found that an interference between the subwaves of the ionizing electron emerging from the different atomic centers lead in most of the molecules to an effective suppression of the ion yields. Below, we will confirm these results by presenting several examples. Molecules studied here include homo- and heteronuclear diatomics, linear triatomics, hydrocarbons, benzene derivatives, chlorinated and fluorinated benzenes, biomolecules, and fullerenes. Independent of the atomic structure we find in general (with the exception of N_2) a suppression of the molecular ionization yield due to the above-mentioned interference effects.

2. S-MATRIX THEORY OF MOLECULAR IONIZATION

Our results are obtained within the so-called strong-field approximation (SFA), which is the leading order term of a S-matrix expansion [2, 19, 20]. It involves a transition matrix element between the initial state wavefunction of the bound state of the molecule, $|\Phi_i\rangle$ and the product state of the Volkov wavefunction $|\phi_{k_N}\rangle$ of the emitted electron in the field [26] and the unperturbed final bound state wavefunction of the residual molecular ion, $|\Phi_f\rangle$. The total rate of ionization from an active orbital with N_e equivalent electrons from a linearly polarized laser field is given by [22]:

$$\Gamma(I) = 2\pi N_e C_{\text{coul}}^2(Z, E_B, E_0) \times \sum_{N=N_0}^{\infty} \int d\hat{\mathbf{k}}_N k_N (U_p - N\omega)^2 J_N^2\left(\alpha_0 \cdot \mathbf{k}_N, \frac{U_p}{2\omega}\right) \times |\langle \phi_{\mathbf{k}_N}(\mathbf{r}_m)\Phi_f(\mathbf{r}_1, \ldots, \mathbf{r}_{m-1}; \{\mathbf{R}\}_j)|\Phi_i(\mathbf{r}_1, \ldots, \mathbf{r}_m); \{\mathbf{R}\}_j\rangle|^2, \quad (1)$$

where the set of coordinates $\{\mathbf{R}\}_j$ denotes the positions of the nuclei in the molecules, E_0 is the peak field strength of the laser and E_B is the ionization potential of the molecule. $J_N(a; b)$ is a generalized Bessel function, where $\alpha_0 = \sqrt{I}/\omega$ is the quiver radius and $U_p = I/4\omega^2$ is the quiver energy of an electron in a laser field of frequency ω and intensity I. $k_N^2/2 = N\omega - U_p - E_B$ is the kinetic energy of an electron on absorption of N photons from the field.

The rate has been corrected approximately for the long-ranged Coulomb interaction between the electron and the residual ion in the final state by the correction factor C_{coul}, derived and proposed initially for the atomic case [27, 28]. For molecules we, in general, adopt the atomic version of the factor $C_{\text{coul}}^2 = (4E_B/E_0 r_B)^{2Z/k_B}$, where $r_B = 2/k_B$ with $k_B = \sqrt{2E_B}$, while for fullerenes we modify the Coulomb factor such that the large but finite size of the fullerene cage is considered and replace r_B by $R + \delta a$, where R is the radius of the fullerene cage and $\delta a(\approx 2/k_b)$ is the spill-out radius of the electron cloud [24].

We have found in our calculations of the total rate, that, in general, the contributions from the nonactive electrons (1, ..., $m-1$) can be neglected in the overlap matrix element between the initial and final wavefunctions. We therefore approximate

$$\langle \phi_{\mathbf{k}_N}(\mathbf{r}_m)\Phi_f(\mathbf{r}_1, \ldots, \mathbf{r}_{m-1}; \{\mathbf{R}\}_j)|\Phi_i(\mathbf{r}_1, \ldots, \mathbf{r}_m; \{\mathbf{R}\}_j)\rangle \approx \phi_{\mathbf{k}_N}\langle \mathbf{r}_m; \{\mathbf{R}\}_j|\phi_i(\mathbf{r}_m; \{\mathbf{R}\}_j)\rangle, \quad (2)$$

where $\phi_i(\mathbf{r})$ denotes the active molecular orbital (usually the highest occupied molecular orbital, HOMO), which can be further expanded into atomic orbitals using the method of linear combination of atomic orbitals (LCAO) as

$$\phi_i(\mathbf{r}) = \sum_{i=1}^{n}\sum_{l=1}^{l_{\max}} a_{i,l}\phi_{i,l}(\mathbf{r}, \{\mathbf{R}\}_j), \quad (3)$$

where n is the total number of nuclei in the molecule, $a_{i,l}$ are the variational coefficients of the atomic basis functions $\phi_{i,l}$ and $l_{\max}$ denotes the size of the basis set used. In all calculations we have used Gaussian basis functions. Consequently Eq. (1) can be written in the form

$$\Gamma(I) = 2\pi N_e C_{\text{coul}}^2(Z, E_B, E_0) \times \sum_{N=N_0}^{\infty} \int d\hat{\mathbf{k}}_N k_N (U_p - N\omega)^2 J_N^2\left(\alpha_0 \cdot \mathbf{k}_N, \frac{U_p}{2\omega}\right) \times \left|\sum_{i=1}^{n} M_i(\mathbf{k}_N, \{\mathbf{R}\}_j)\right|^2, \quad (4)$$

where

$$M_i(\mathbf{k}_N, \{\mathbf{R}\}_j) = \sum_{l=1}^{l_{\max}} a_{i,l}\langle \phi_{\mathbf{k}_N}(\mathbf{r})|\phi_{i,l}(\mathbf{r}, \{\mathbf{R}\}_j)\rangle. \quad (5)$$

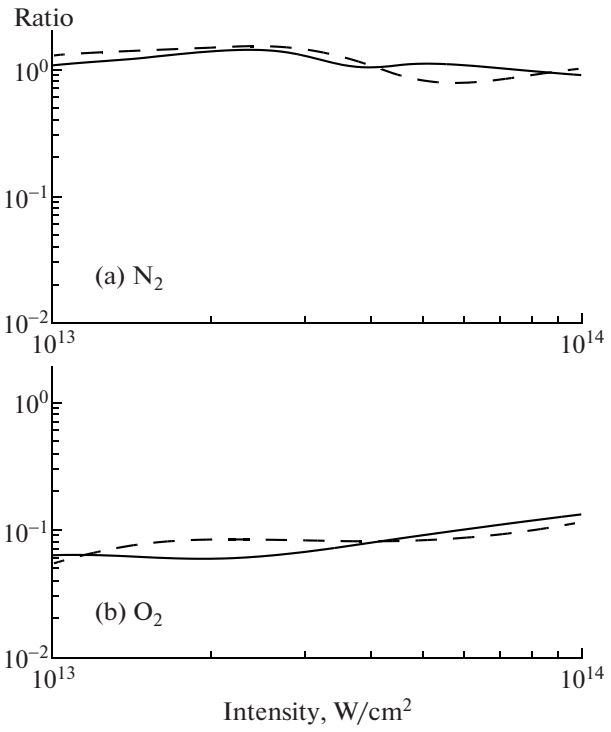

Fig. 1. Ratio of total ion yields obtained using the full coherent calculation to those obtained within the incoherent sum approximation as a function of the peak laser intensity. (a) N_2 at 600 (dashed line) and 800 nm (solid line) and (b) O_2 at 600 (dashed line) and 800 nm (solid line). The pulse length was 50 fs.

We may note, that the above formula holds for atoms too and its tunneling limit is related to the quasistatic ionization rates, derived in the 1960s and hence to the ADK formula as well. Equation (4) shows however the important difference to the atomic case, namely that the total ionization rate is proportional to modulus square of the coherent sum of contributions from atomic orbitals. It is therefore the multi-center character of the wavefunction of the molecule which leads to a multi-slit like interference of the partial waves arising from the coherent sum of partial amplitudes in the matrix element $M_i(\mathbf{k}_N, \{\mathbf{R}\}_j)$. This coherent sum is obviously absent in the atomic case.

To study the role of the interference effects on the ionization signals we also consider the incoherent sum of the atomic contributions via the following approximation

$$\left|\sum_{i=1}^{n} M_i(\mathbf{k}_N, \{\mathbf{R}\}_j)\right|^2 \approx \sum_{i=1}^{n} \left|M_i(\mathbf{k}_N, \{\mathbf{R}\}_j)\right|^2, \qquad (6)$$

that is the modulus square of the coherent sum of partial amplitudes is replaced by the *incoherent* sum of their squares. The corresponding total ionization rate

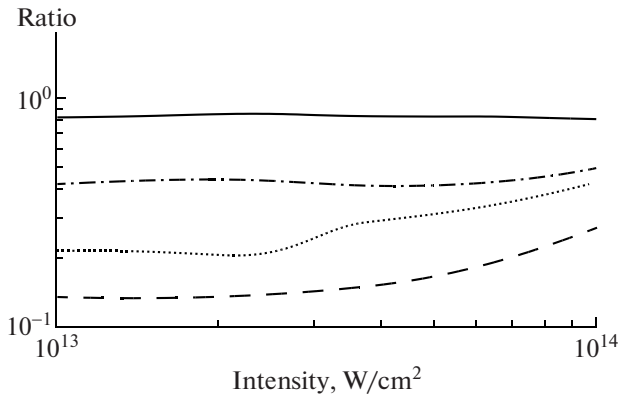

Fig. 2. Same as Fig. 1, but for CO (solid line), CO_2 (dashed line), NO (dotted line), and NO_2 (dashed-dotted line) at a laser wavelength of 800 nm and a pulse length of 50 fs.

in this *incoherent sum approximation* (ISA) is given therefore given by:

$$\Gamma_{\mathrm{ISA}}(I) = 2\pi N_e C^2_{\mathrm{coul}}(Z, E_B, E_0) \times \sum_{N=N_0}^{\infty} \int d\hat{\mathbf{k}}_N k_N (U_p - N\omega)^2 J_N^2\left(\boldsymbol{\alpha}_0 \cdot \mathbf{k}_N, \frac{U_p}{2\omega}\right) \times \sum_{i=1}^{n} \left|M_i(\mathbf{k}_N, \mathbf{R}_i)\right|^2. \qquad (7)$$

From both the rates, in the full calculation (Eq. (4)) and in the incoherent sum approximation (Eq. (7)), we have obtained ion yields by combining the rate formula with the respective rate equations as follows,

$$\frac{dP(\mathbf{r}, t)}{dt} = \Gamma(I(\mathbf{r}, t))(1 - P(\mathbf{r}, t)), \qquad (8)$$

where $I(\mathbf{r}, t)$ is the space-time profile of the laser beam. The rate equations are solved under the constraints $P(\mathbf{r}, t = -\infty) = 0$ respectively, and the contributions from all points in the laser focus are summed up. For the actual computations we have used a Gaussian pulse profile, centered around $t = 0$, and a TEM_{00}-mode Gaussian beam with pulse length equal to 50 fs.

In the following we shall present results for the ratio of the total ion yield obtained using the full coherent sum calculation, Eq. (4), to the total ion yield obtained assuming ISA. This ratio elucidates the role of the (destructive) interference effects on the ionization signals originating from different atoms of the multi-center wavefunction. We have considered a series of di- and polyatomic molecules with different geometric structures. The geometries of the molecules were optimized within the Quadratic Configuration Interaction (QCISD) method [29], whereas equilibrium geometries for fullerenes were optimized using the Density Functional Tight–Binding (DFTB) method [30], which allows very efficient simulation

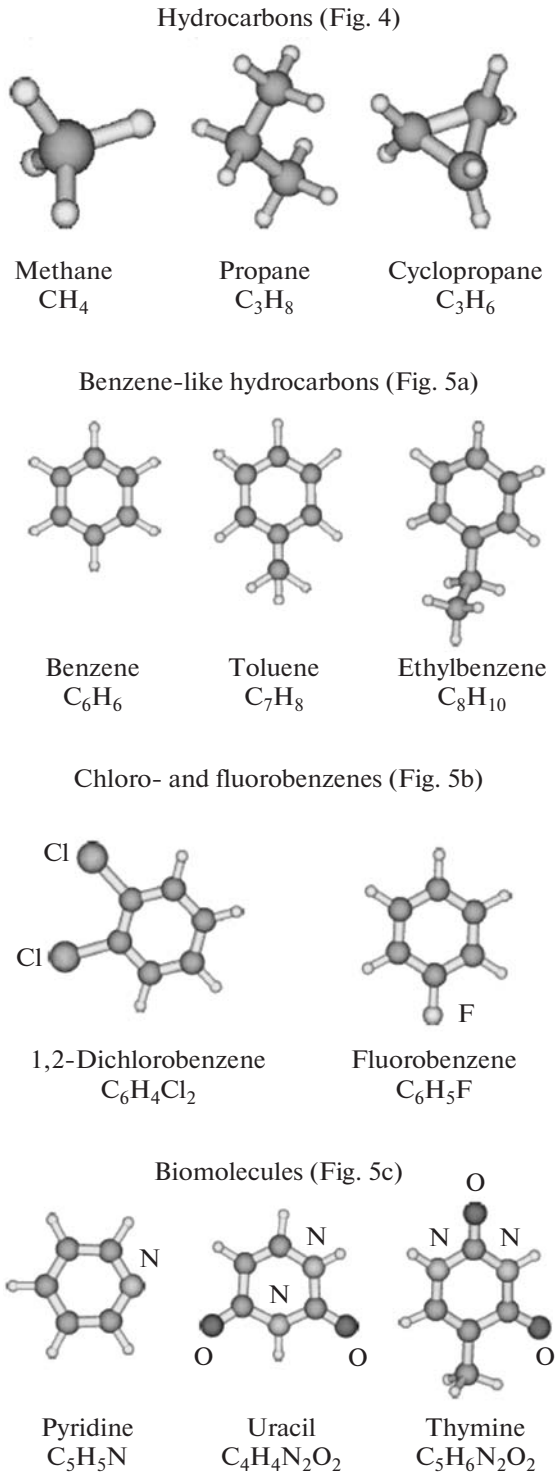

Fig. 3. Geometries of polyatomic molecules considered in the present study.

for larger molecules. The wavefunction for equilibrium geometry of fullerenes were then calculated within Hartree–Fock (HF) (for fullerenes) or QCISD (for other molecules) methods. All results were obtained after averaging over the orientation of the molecules with respect to the polarization direction of the laser.

3. SMALL MOLECULES

In this section we study a number of small molecules, namely di- and triatomics. In all cases presented below we have considered interaction of the molecule with a Ti:sapphire laser operating at 600 and 800 nm and having a pulse length (FWHM) of 50 fs. Intensities are varied such that in the full calculations the range of intensities is below the respective saturation intensity. We will present in this and the next section ratios of the total ion yield obtained using the full coherent sum to the total ion yield obtained using the incoherent sum approximation. If the presented ratio is below one, as in most of the cases presented here, the interference effect arising from the partial electron waves is destructive and, hence, contributes to a suppression of the ion yield.

3.1. Homonuclear Diatomics N_2 and O_2

We first consider the homonuclear diatomics N_2 and O_2. The HOMO orbitals of N_2 and O_2 have correspondingly bonding (σ_g) and antibonding (π_g) symmetry. It has been shown [22, 31] that in case of a σ_g orbital the leading term of the coherent sum of the partial amplitudes, Eq. (5), is proportional to $\cos(\mathbf{k}_N \cdot \mathbf{R}/2)$, where $\mathbf{R}$ is the internuclear distance between the two nuclei. In contrast, for a π_g-orbital the leading term is proportional to $\sin(\mathbf{k}_N \cdot \mathbf{R}/2)$. These molecular structure effects therefore lead to an effective suppression of the low-energy part of the above threshold ionization spectrum [31] and, hence, to a suppression of the total ion yield [22] in case of a π_g-orbital (O_2), but not for a σ_g orbital (N_2), which corresponds to the experimental observations [9, 10, 31].

The effects of non-suppression in the case of (a) N_2 and suppression for (b) O_2 can be readily seen from the ratios of ion yields obtained using the full coherent calculation and the incoherent sum approximation presented in Fig. 1. At both laser wavelengths of 600 nm (dashed lines) and 800 nm (solid line) the interference effects lead to a suppression of the ion yields of about an order of magnitude in case of the oxygen molecule, while the effect on the yields for the nitrogen molecule are small. Further examples of the interference effect for different orbital symmetries in diatomics have been presented in [32, 33].

3.2 Heteronuclear Di- and Triatomics

Next we consider heteronuclear diatomics, namely CO, NO, CO_2, and NO_2. The corresponding ratios obtained at a wavelength of 800 nm are shown in Fig. 2. It is obvious that in all cases the interference

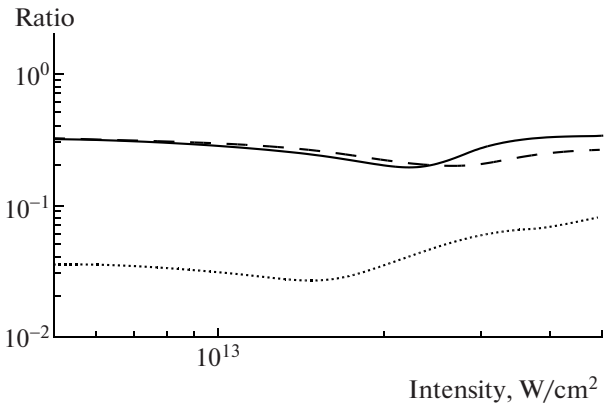

Fig. 4. Same as Fig. 1, but for the hydrocarbons methane (solid line), propane (dashed line), and cyclopropane (dotted line) at 800 nm and 50 fs.

effect is destructive and leads to a suppression of the ion yields of the molecules, since the presented ratios are smaller than one at all intensities for each of the molecules.

The suppression is of different strength for the individual molecules, which can be understood from the structure and symmetry of the respective HOMOs. For CO (solid line) the HOMO is of σ_g-symmetry, as in case of N_2. Since CO is a heteronuclear molecule the (constructive) interference between the two electron sub-waves emanating from the two atomic centers is not perfect (due to the asymmetry of the orbital over the two nuclei). As a result, a but weak suppression of the ion yield is found, visualized in Fig. 2 via a ratio smaller but close to one. A similar degree of suppression for CO, as compared to its companion atom Kr, has been found in the experiment by Chin and Talebpour [12].

Strongest suppression among the results presented in Fig. 2 is found for ionization from the HOMO of CO_2 (dashed line), which has π_g-symmetry as O_2. Indeed, in the electronic wavefunction for the HOMO of CO_2 the contributions at the central C atom are negligible and the molecule acts as an elongated homonuclear O_2 molecule. The suppression of the total ion yields is therefore strong (small ratio in Fig. 2) but slightly weaker than for O_2 since the (effective) internuclear distance between the two O atoms is larger in CO_2 than in O_2.

The HOMO of NO has π_g-symmetry too, due to the heteronuclear character of the molecule the suppression is not as effective as in O_2 and CO_2 and the corresponding ratio (dotted line in Fig. 2) is larger but still clearly below one. Finally, NO_2 has a bent geometrical structure and symmetry arguments are not as obvious as in the case of diatomics and linear polyatomics (for the latter, see [33]). However, the ratio for NO_2 (dashed-dotted line) is clearly below one showing

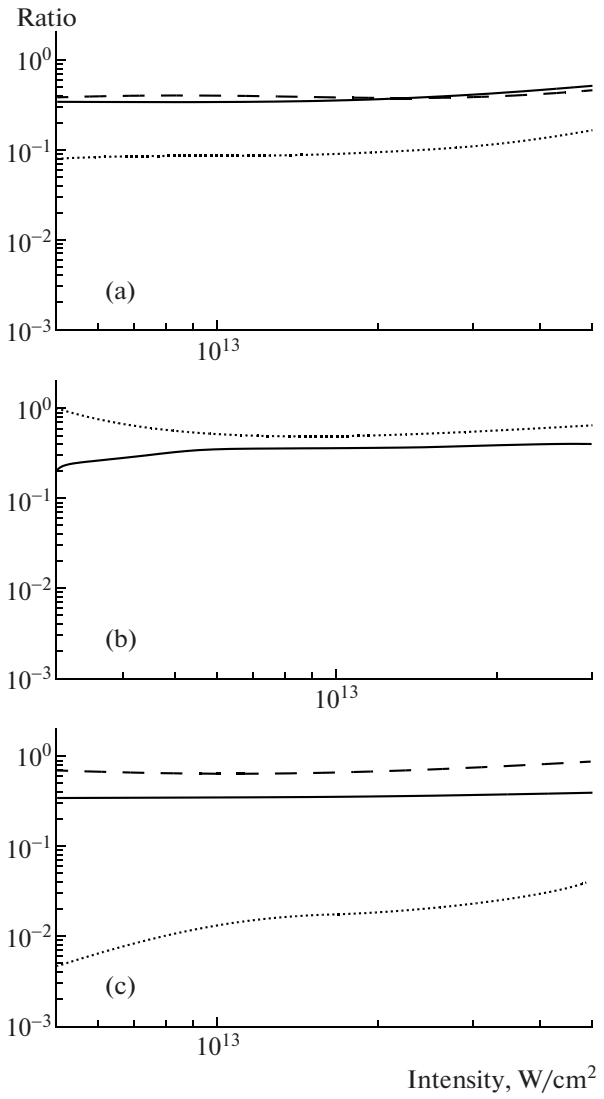

Fig. 5. Same as Fig. 1, but for (a) benzene (solid line) and benzene derivatives toluene (dashed line) and ethylbenzene (dotted line); (b) 1,2-dichlorobenzene (solid line) and fluorobenzene (dashed line); (c) uracil (solid line), thymine (dotted line) and pyridine (dashed line) at 800 nm and 50 fs.

that interferences lead to an effective suppression of the ion yield for this molecule too.

Before we proceed we may comment on a subtle aspect of some of the ratios presented in Fig. 2 and other Figures below. For some of the molecules (CO_2, dashed line, and NO, dotted line, in Fig. 2) the ratio of the total ion yields show an increase towards higher laser intensities. As outlined at the outset of this section we have considered laser intensities below the respective saturation intensity for the total ion yields obtained in the full *coherent* sum calculation. These rates are (strongly) suppressed due to interference effects, or vice versa, those obtained in the incoherent sum approximation are strongly enhanced. Conse-

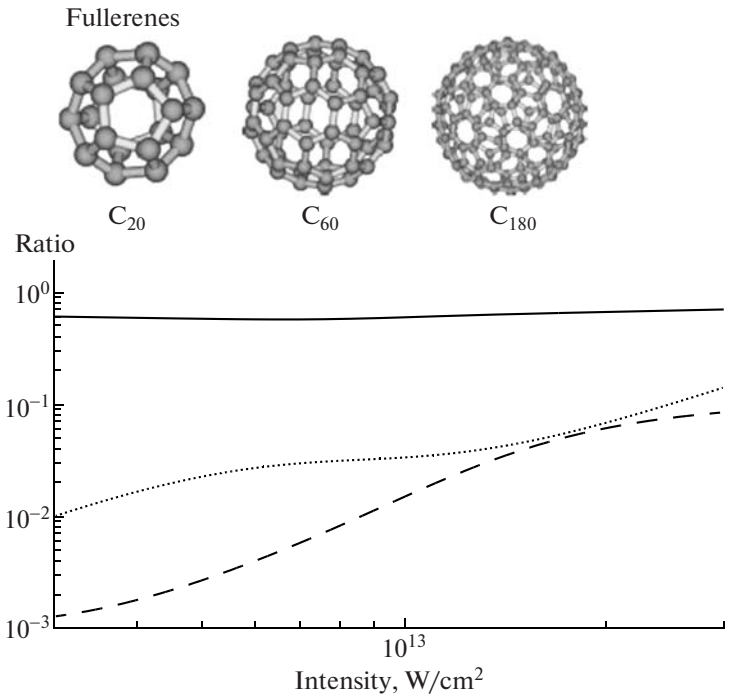

Fig. 6. Upper row: Geometrical structure of the three fullerenes studied. Lower row: same as Fig. 1, but for C_{20} (solid line), C_{60} (dashed line), and C_{180} (dotted line) at 800 nm and 50 fs.

quently, in the incoherent sum approximation saturated ionization is reached at lower intensities already. Since an ion yield, in general, increases below the saturation at a higher rate than above saturation, the ratios have to increase beyond the saturation intensity for the ion yields obtained in the incoherent sum approximation.

4. COMPLEX MOLECULES: FROM HYDROCARBONS TO FULLERENES

In this section we consider the suppression of molecular ionization by interference effects due to the coherent sum of the partial amplitudes from the different atomic centers in a more general way. To this end, we have chosen 11 complex molecules, ranging from small hydrocarbons via different benzene-like hydrocarbons, clorinated and fluorinated benzenes to biomolecules, and three fullerenes with icosahedral geometric structure. The molecules have different geometrical structures (see Fig. 3 for the equilibrium geometries) with just one central C atom (methane) or benzene-like ring structures with or without partial substitution of one or two carbon atom. Our intention is to investigate whether the suppression of molecular ionization due to interference effects, observed above for small molecules too, is effective for more complex molecules, independent of their geometrical structure. The suppression is, in general, indeed present in all of the cases investigated. We will, however, not discuss the degree of suppression for the individual molecule in detail in this general overview.

In Fig. 4 we present the ratios of the total ion yields for the three hydrocarbons methane (solid line), propane (dashed line) and cyclopropane (dotted line). The suppression due to interference is present in all cases and strongest (smallest ratio in Fig. 4) for cyclopropane. This might be due to the cyclic structure of cyclopropane as compared to the bent structure of propane and the structure with a single central C atom in methane.

Next, we have considered a series of molecules, which have a similar geometric structure as the benzene molecule (solid line in Fig. 5a). These molecules have either additional CH_n groups (toluene and ethylbenzene in Fig. 5a), substituted one or two of the H atoms by Cl (1,2-diclorobenzene in Fig. 5b) or F atoms (fluorobenzene in Fig. 5b) or substituted one or more of the C atoms by O and/or N atoms (pyridine, uracil and thymine in Fig. 5c).

Again, in all the cases we find ratios below one, indicating a suppression of ionization due to interference effects in each of the molecules. There is however no clear trend visible related to the geometrical structure of these molecules. From simple symmetry consideration one may expect the strongest interference effects for molecules with a highly symmetric geometric structure. But, for example, the addition of a CH_n group in toluene leads to a stronger suppression of the ion yield, as compared to benzene. On the other hand,

ethylbenzene (having added another CH_n group) shows a similar degree of suppression as benzene. Similar observations can be made for the group of biomolecules, shown in Fig. 5c, thymine shows the strongest suppression in the ion yield despite the fact that is has the geometric structure with the lowest symmetry out of the three biomolecules.

Finally, in Fig. 6 we present the respective ratios for three fullerenes with icosahedral symmetry C_{20} (solid line), C_{60} (dashed line), and C_{180} (dotted line). Clearly, there is a strong suppression due to interferences found for the two larger fullerenes, but a weak suppression is present for C_{20} too. This corresponds to the results of our previous analysis of the saturation intensities of these fullerenes [24, 25]. It has been shown before, that in case of the fullerenes besides the interference effects the large fullerene radius (and the corresponding smaller Coulomb effect) explains the observed strong suppression of the corresponding saturation intensities as compared to the predictions of the atomic ADK theory [18, 24]. We may finish by mentioning that the interference effects are predicted [34, 35] to show up as pronounced minima in the high harmonic spectra generated in these molecules and might be used to image laser induced changes of the radius of the fullerene cage.

5. CONCLUSIONS

We have studied the role of interference effects arising from the sub-waves of the emitted electron in the ionization of molecules in strong laser fields. It is found that these interference effects, in general, lead to a suppression of the ionization rate and the ion yield. Thus, they provide a qualitative explanation of the phenomenon of suppressed molecular ionization as compared to the prediction of the atomic ADK theory.

ACKNOWLEDGMENTS

We acknowledge many stimulating discussions and support by F.H.M. Faisal, S.L. Chin, J. Muth-Böhm, and M.F. Ciappina on this topic.

REFERENCES

1. H. A. Bethe and E. E. Salpeter, *Quantum Mechanics of One- and Two-Electron Atoms* (Plenum, New York, 1977).
2. L. V. Keldysh, Sov. Phys. JETP **20**, 1307 (1965).
3. A. M. Perelomov, S. V. Popov, and M. V. Terent'ev, Sov. Phys. JETP **23**, 924 (1966).
4. M. V. Amossov, N. B. Delone, and V. P. Krainov, Sov. Phys. JETP **64**, 1191 (1986).
5. S. L. Chin, F. Yergeau, and P. Lavigne, J. Phys. B **18**, L213 (1985).
6. F. Yergeau, S. L. Chin, and P. Lavigne, J. Phys. B **20**, 723 (1987).
7. S. Augst, D. Strickland, D. D. Meyerhofer, S. L. Chin, and J. H. Eberly, Phys. Rev. Lett. **63**, 2212 (1989).
8. T. D. G. Walsh, F. A. Ilkov, J. E. Decker, and S. L. Chin, J. Phys. B **27**, 3767 (1994).
9. A. Talebpour, C.-Y. Chien, and S. L. Chin, J. Phys. B **29**, L677 (1996).
10. C. Guo, M. Li, J. P. Nibarger, and G. N. Gibson, Phys. Rev. A **58**, R4271 (1998).
11. A. Talebpour, S. Larochelle, and S. L. Chin, J. Phys. B **31**, L49 (1998).
12. A. Talebpour, PhD Thesis (Université Laval, Québec, 1998).
13. A. Talebpour, S. Larochelle, and S. L. Chin, J. Phys. B **31**, 2769 (1998).
14. S. M. Hankin, D. M. Villeneuve, P. B. Corkum, and D. M. Rayner, Phys. Rev. Lett. **84**, 5082 (2000).
15. S. M. Hankin, D. M. Villeneuve, P. B. Corkum, and D. M. Rayner, Phys. Rev. A **64**, 013405 (2001).
16. A. Talebpour, S. Larochelle, and S. L. Chin, J. Phys. B **31**, 2769 (1998).
17. H. Harada, M. Tanaka, M. Murakami, S. Shimizu, T. Yatsuhashi, N. Nakashima, S. Sakabe, Y. Izawa, S. Tojo, and T. Majima, J. Phys. Chem. A **107**, 6580 (2003).
18. V. R. Bhardwaj, P. B. Corkum, and D. M. Rajner, Phys. Rev. Lett. **91**, 203004 (2003).
19. F. H. M. Faisal, J. Phys. B **6**, L89 (1973).
20. H. R. Reiss, Phys. Rev. A **22**, 1786 (1980).
21. A. Becker and F. H. M. Faisal, J. Phys. B **38**, R1 (2005).
22. J. Muth-Böhm, A. Becker, and F. H. M. Faisal, Phys. Rev. Lett. **85**, 2280 (2000).
23. J. Muth-Böhm, A. Becker, S. L. Chin, and F. H. M. Faisal, Chem. Phys. Lett. **337**, 313 (2001).
24. A. Jaron-Becker, A. Becker and F. H. M. Faisal, Phys. Rev. Lett. **96**, 143006 (2006).
25. A. Jaron-Becker, A. Becker and F. H. M. Faisal, J. Chem. Phys. **126**, 124310 (2007).
26. D. M. Volkov, Z. Phys. **94**, 250 (1935).
27. V. P. Krainov, J. Opt. Soc. Am. B **14**, 425 (1997).
28. A. Becker, L. Plaja, P. Moreno, M. Nurhuda, and F. H. M. Faisal, Phys. Rev. A **64**, 023408 (2001).
29. *Gaussian03, Revision C.02*, (Gaussian, Wallingford, CT, 2004); http://www.gaussian.com.
30. D. Porezag, Th. Frauenheim, Th. Köhler, G. Seifert, and R. Kaschner, Phys. Rev. B **51**, 12947 (1995).
31. F. Grasbon, G. G. Paulus, H. Walther, S. L. Chin, J. Muth-Böhm, A. Becker, and F. H. M. Faisal, Phys Rev. A **63**, 041402(R) (2001).
32. A. Jaron-Becker, A. Becker, and F. H. M. Faisal, J. Phys. B **36**, L375 (2003).
33. A. Jaron-Becker, A. Becker, and F. H. M. Faisal, Phys. Rev. A **69**, 023410 (2004).
34. M. F. Ciappina, A. Jaron-Becker, and A. Becker, Phys. Rev. A **76**, 063406 (2007).
35. M. F. Ciappina, A. Becker, and A. Jaron-Becker, Phys. Rev. A **78**, 063405 (2008).